

1 **Neotectonic deformation in a Scottish fjord, Loch Broom, NW Scotland**

2

3 Martyn Stoker* & Tom Bradwell

4 *British Geological Survey, Murchison House, West Mains Road, Edinburgh, EH9 3LA, UK*

5 (*e-mail: mss@bgs.ac.uk)

6

7 **Synopsis**

8

9 Multibeam bathymetry, boomer seismic profiles and sediment core data from outer Loch
10 Broom reveal slumping of the basin-floor fjord deposits of the Assynt Glacigenic Formation.
11 On the swath image, the expression of slumping is manifest as two distinct sea bed
12 depressions, at least 10 m deep and several hundred metres wide. Although the extent of
13 displacement is constrained within the fjord, the seismic profiles reveal extensional and
14 compressional faulting, and associated folding, within the fjord infill. The possibility that
15 collapse of the sea bed has been partly facilitated by some kind of associated fluid release
16 along the fault planes cannot be discounted. Local (core data) and regional stratigraphical
17 information indicate that slumping occurred shortly after deposition of the Assynt Glacigenic
18 Formation, between about 14 and 13 ka BP, during the deglaciation of the fjord region. It is
19 inferred that these slumps broadly correlate with two areas of major sliding in adjacent fjord
20 basins, and are linked to a regional phase of Lateglacial instability throughout the Summer
21 Isles region. It is suggested that earthquake activity related to ice unloading is the most
22 probable cause of this deformation. Holocene bottom-current activity has partially modified
23 the shape of the depressions, and influenced the nature of the sediment infill.

24

25 **Introduction**

26

27 By virtue of their association with glaciation, fjords are characteristically immature, non-
28 steady state systems, which evolve and change over relatively short time scales (Syvitski &
29 Shaw 1995). They have immense sediment storage capacity and during deglaciation act as
30 efficient sediment traps. Fjords dominated by glacier ice and ice-melt processes experience
31 high rates of sediment accumulation ($>1 \text{ cm yr}^{-1}$, averaged across a fjord basin: Syvitski &
32 Shaw 1995), with the infill commonly displaying a highly variable grain size and size
33 distribution, and is typically underconsolidated (Sangrey *et al.* 1979). Sedimentation in a fjord
34 is often accompanied by exceptional rates of isostatic uplift, which, together with the steep-
35 sided nature of fjord-valley slopes, makes them ideal environments for all kinds of sediment
36 deformation, be it due to gravity of the accumulating deposit or to external stimuli, such as
37 earthquakes. Examples of sediment slides and slumps are to be found in fjords worldwide,
38 including Canada (Syvitski & Hein 1991), East Greenland (Whittington & Niessen 1997;
39 Niessen & Whittington 1997) and Norway (Aarseth *et al.* 1989; Hjelstuen *et al.* 2009).

40

41 Recent work in the Summer Isles region of NW Scotland (Fig. 1) indicates that Scotland's
42 fjords are no exception. Stoker *et al.* (in press) have identified an up to 100 m thick sequence
43 of fjord sediments, which were deposited during the landward retreat of the ice margin from
44 the Summer Isles into the present-day sea lochs of Loch Broom and Little Loch Broom, and
45 eventually into the adjacent onshore valleys. It is calculated that the basin-wide sediment
46 accumulation rate was as high as 10 cm/yr during the deposition of the fjord infill. Swath
47 bathymetric imagery and high-resolution seismic reflection data have shown that mass failure
48 is pervasive throughout the Summer Isles region, and two large-scale sediment slides, the
49 Little Loch Broom Slide Complex and the Cadail Slide (Fig. 1), have been recognised (Stoker

50 *et al.* 2006, in press; Wilson *et al.* in press). In both of these features, sliding has occurred
51 from the sides of the fjords into the adjacent basinal area. In this paper, we report a different
52 style of deformation that has affected the fjord fill in the outer part of Loch Broom, but where
53 the sea-bed expression of deformation is confined to the relatively flat-lying floor of the fjord.
54 Geophysical and geological data are used to determine the style and geometry of the
55 deformation, as well as to provide constraints on its timing. Considered together with the
56 regional pattern of neotectonic deformation, the structures in Loch Broom may provide a clue
57 as to the stability of the ice-influenced hinterland during the Lateglacial interval.

58

59 **Study area and glacial geology**

60

61 Loch Broom is a 15 km long sea loch located on the NW seaboard of Scotland (Fig. 1). It
62 ranges in width from 0.5 to 1.5 km, and in water depth from <20 m offshore from Ullapool,
63 up to 90 m near the mouth of the loch. The inner loch (SE of Corry Point) is everywhere
64 shallower than 60 m water depth. The seaward extension of Loch Broom continues as a series
65 of overdeepened basins (locally >150 m in water depth) that trend south of Cadail Bank and
66 through Annat Bay towards the Summer Isles (Stoker *et al.* 2006, in press) (Fig. 1).

67

68 The depth to bedrock in Loch Broom is locally at 180 m below OD in the outer loch. To the
69 west of Corry Point, bedrock is dominated by Neoproterozoic Torridonian sandstone with
70 sporadic inliers of Archaean gneiss, though a thin strip of Cambro-Ordovician rocks between
71 Ullapool and the Moine Thrust extends along the line of the thrust zone. Moine Supergroup
72 rocks overlie these strata to the east of the Moine Thrust. Structural control on the alignment
73 of the fjords seems likely. NW-trending faults are a major component of the bedrock geology
74 in NW Scotland, and a fault is known to run along Little Loch Broom (British Geological

75 Survey, 1998). Fault control of Loch Broom is also deemed probable, especially given the
76 elongate nature of the adjacent offshore banks (Fig. 1). The intersecting pattern of NE- and
77 NW-trending faults has resulted in the compartmentalisation of the bedrock, essentially into a
78 series of blocks.

79
80 The glacial geology of the area is summarised in Figure 2 and Table 1; for details see Stoker
81 *et al.* (in press). All dates have been calibrated (Fairbanks *et al.* 2005) and are expressed as
82 calendar years (ka BP). The major part of the succession records a time transgressive
83 landward retreat of the Lateglacial ice margin from the Summer Isles back to the sea lochs of
84 Loch Broom and Little Loch Broom. Ice-contact to ice-proximal glacimarine and ice-distal
85 glacimarine facies, assigned to the Assynt Glacigenic and Annat Bay Formations respectively,
86 comprise the bulk of the sediment infilling the fjord region. Cosmogenic isotope surface
87 exposure ages of boulders from onshore moraines of the Assynt Glacigenic Formation,
88 combined with radiocarbon dating of marine shells from, and micropalaeontological analysis
89 of, both the Assynt Glacigenic and Annat Bay Formations in offshore sediment cores suggests
90 that these units were deposited largely between about 14 and 13 ka BP, i.e. during the
91 Lateglacial Interstadial (Bradwell *et al.* 2008; Stoker *et al.* in press). Within Loch Broom,
92 late-stage oscillation of valley glacier lobes back into the fjord correlates with several discrete
93 Late-stage members of the Assynt Glacigenic Formation (Fig. 2). An associated series of fan-
94 deltas comprise the Ullapool Gravel Formation, which is sandwiched between these Late-
95 stage members. As the fjord gradually became free of ice, the Outer and Inner Loch Broom
96 shell beds accumulated as a time-transgressive deposit on the floor of the fjord. The Inner
97 Loch Broom shell bed is overlain by glacial diamicton in the inner loch, which provides an
98 age constraint of <13 ka BP for the ice-margin oscillation within the inner fjord (Stoker *et al.*
99 in press). The Late-stage debris flows represent a discrete lithogenetic unit that occurs

100 sporadically throughout the Summer Isles region. This unit post-dates the Assynt Glacigenic
101 and Annat Bay Formations, but pre-dates the Summer Isles Formation, which forms a cover
102 of Holocene marine sediments deposited after about 8 ka BP (Stoker *et al.* in press). The
103 deformed sediments described in this paper are assigned to the Assynt Glacigenic Formation.

104

105 **Methods**

106

107 This study combines geophysical and geological data collected by the British Geological
108 Survey (BGS) in the Summer Isles region between 2005 and 2007. A marine geophysical
109 survey of the Summer Isles region, including Loch Broom, was undertaken in July 2005, and
110 acquired multibeam swath bathymetry and high-resolution seismic reflection data (Stoker *et*
111 *al.* 2006). Bathymetric data were acquired using a GeoSwath system operating at 125 kHz,
112 mounted on a retractable bow pole on the *R/V Calanus*. Swath survey lines were traversed at a
113 spacing of 200 m, thereby enabling swath overlap and full coverage bathymetry across an area
114 of 225 km². The data were collected on a GeoSwath computer with post-acquisition
115 processing carried out on a separate workstation. Output was in the form of xyz data with a
116 typical grid spacing of 3 m. The grid was converted into a depth-coloured shaded-relief image
117 using Fledermaus (processing and visualisation software). The shaded-relief image of the
118 study area is shown in Figure 3. The seismic reflection data were acquired using a BGS-
119 owned Applied Acoustics surface-towed boomer and hydrophone. Fifty-seven boomer
120 profiles (a total length of about 235 km) were collected across the region; profiles relevant to
121 this study are BGS05/04-37, 47 and 48 (Fig. 4). The data were recorded and processed (Time
122 Varied Gain, Bandpass Filter 800–200 Hz) on a CODA DA200 seismic acquisition system
123 and output as SEG-Y and TIFF format. Further technical details of the geophysical data
124 collection are outlined in Stoker *et al.* (2006).

125

126 On the basis of regional measurements of superficial sediments offshore from Scotland, sound
127 velocities in the fjord sediment fill are taken to be in the range of 1500–2000 ms⁻¹ depending
128 upon their composition and degree of induration (McQuillin and Arduis 1977; Stoker *et al.*
129 1994). In this paper, the conversion of sub-bottom depths from milliseconds to metres has
130 been generally taken as a maximum estimate (i.e. 20 msec two-way travel time (TWTT) ≤20
131 m) of sediment thickness. However, for high-resolution correlation between the boomer
132 profiles and the sediment cores in the basinal areas, a sound velocity of 1500–1600 ms⁻¹ is
133 most appropriate. The relief of features with expression at the sea bed is based on the sound
134 velocity in water of 1450 ms⁻¹ (Hamilton 1985).

135

136 Geological calibration of the geophysical data was established using BGS vibrocore 57-
137 06/269, which was collected in September 2007, using the *R/V James Cook*. This core is here
138 described in terms of its lithology and sedimentary structure. Stratigraphic correlation of this
139 core is based on a regional study of all cores collected in the Summer Isles region (a total of
140 50 sample stations), which is detailed in Stoker *et al.* (in press).

141

142 **Results**

143

144 Swath bathymetry

145

146 The multibeam swath bathymetry data reveal two distinct sea bed depressions on the floor of
147 outer Loch Broom, which are labelled A and B (Fig. 3). Figure 3a presents a perspective view
148 looking towards the mouth of Loch Broom; Figure 3b shows the planform view together with
149 an interpretation of the image. The floor of feature A is 10 m deeper (90 m below OD) than

150 the surrounding sea bed, and is 200–300 m wide. Slope angles within the depression vary
151 from 5–10°. It displays a broadly rectilinear outline, though the northern corner of the feature
152 appears to be elongated towards the northern slope of the loch (Ai in Fig 3b). This projection
153 is about 75 m in width, with its floor just 1–2 m below the adjacent sea bed. The southern
154 margin of the feature is marked by a slight bathymetric rise of the sea bed of about 1 m over a
155 distance of 100 m (Aii in Fig. 3b). The broad outline of feature B is not dissimilar to A, albeit
156 more diffuse, in that it delineates a broad depression up to 350 m across. However, within the
157 depression the sea bed is shaped into a series of discrete circular to ovoid hollows separated
158 by an area of positive bathymetric relief. The deepest hollows occur on the outer side of the
159 feature (Fig. 4a), and are between 5 and 10 m deep; the shallower hollows are just 1–2 m
160 deep. The area of positive relief that separates these hollows is generally deeper (by 2–4 m)
161 than the general level of the surrounding basin floor.

162

163 High-resolution seismic reflection data

164

165 The sea bed depressions (A & B) are variably intersected by BGS boomer profiles 05/04-37,
166 47 and 48 (Fig. 4), which illustrate the sub-sea bed glacial geology of the outer part of Loch
167 Broom. From these profile data, the steep sides of the fjord are clearly defined by a high-
168 amplitude reflecting surface that here descends to about 150 to 160 m below OD. The smooth
169 sides of the fjord are probably composed of bedrock; however, this reflecting surface becomes
170 more irregular towards its base. This may be indicative of basal lodgement till associated with
171 the Loch Broom Till Formation (Fig. 2), or diamicton derived by mass failure from the
172 sidewalls of the fjord prior to the deposition of the overlying Assynt Glacigenic Formation,
173 which is characterised by an acoustically well-layered, ponded seismic reflection
174 configuration. At the study site, the Assynt Glacigenic Formation is overlain by the thin Outer

175 Loch Broom shell bed (not seismically distinguishable, but see Fig. 5) and the Summer Isles
176 Formation, which generally displays a weaker acoustically layered signature, but is
177 characteristically moulded into a cover of variable thickness that forms a partial to almost-
178 total infill of the depressions (Figs 4b & 4c). Within the depressions, an acoustically-
179 structureless infill occurs at the base of the Summer Isles Formation. At the mouth of Loch
180 Broom, adjacent to Cadail Bank, a Late-stage debris flow deposit is sandwiched by the Assynt
181 Glacigenic and Summer Isles Formations (Figs 2 & 4, Table 1).

182

183 The most striking observations from the profile data are that: 1) the Assynt Glacigenic
184 Formation is faulted and folded in the vicinity of the depressions; and, 2) the depth of the
185 depressions extends deeper (by up to 10 m) than their current bathymetric expression. The
186 fault style varies from planar to curved, the latter locally developing a listric expression that
187 may penetrate the entire Assynt Glacigenic Formation (Figs 4a & 4b). Faulting is
188 predominantly of an extensional nature, with offsets of up to a few metres, and downthrow
189 mainly to the southeast. At the seismic scale, there is no obvious change in layer thickness
190 across a fault. A rollover anticline is noted in Figure 4b. On the southern flank of feature A,
191 profile 05/04-37 shows upward diverging faults that are associated with the development of a
192 compressional anticlinal structure, which has raised the level of the sea bed locally (Fig. 4a).
193 This complements a syncline that, on the profile, has an apparent amplitude of about 10 m,
194 with a wavelength of about 200 m. The compressional structure appears to have developed
195 adjacent to an intrabasinal high, formed either of bedrock, lodgement till or a sidewall-derived
196 mass failure deposit. The synclinal form is more enhanced on profile 05/04-48, which
197 transects feature A centrally, and shows the original surface of the depression to extend to
198 about 20 m below the surrounding sea bed (Fig. 4b). Reverse faulting is also observed on this
199 profile, adjacent to the northern side of the loch where the sea bed profile is gently arched. No

200 comparable fold pair is observed with feature B, though significant faulting underlies the
201 depression, and a gentle monoclinial flexure is observed on its southern flank (Fig. 4c).
202 Truncation of the uppermost reflections within the Assynt Glacigenic Formation is noted on
203 the margin of both depressions, the buried surface of which is locally angular (Figs 4b & 4c).
204
205 The faults do not penetrate into the overlying stratigraphic units. The Late-stage debris flow
206 and the Outer Loch Broom shell bed (see below: Fig. 5) both rest with sharp, irregular, eroded
207 contact on the faulted Assynt Glacigenic Formation, whereas the Summer Isles Formation
208 forms a cover of variable thickness on all of the underlying sediments. Both profiles across
209 feature A indicate that the original disposition of the depression is largely retained despite
210 partial infill by predominantly Summer Isles Formation deposits (Figs 4a & 4b). In contrast,
211 the cover of younger deposits that overlies the original surface of feature B is moulded into a
212 series of highs and lows, with the deepest part of the depression underlying an area of positive
213 bathymetric relief (Fig. 4c). This is a very significant observation in that it indicates that the
214 discrete and separate hollows enclosed within feature B are not directly related to the feature
215 itself; instead, profile 05/04-47 (Fig. 4c) shows that they are specifically associated with the
216 Summer Isles Formation, and are thus most likely related to the processes responsible for the
217 differential nature of its thickness.

218

219 Core data

220

221 BGS vibrocore 57-06/269 sampled 4.96 m into the fjord succession in outer Loch Broom,
222 with the Assynt Glacigenic Formation penetrated at a depth of 1.0 m (Fig. 5). In this core, this
223 unit is composed of very soft to soft, colour-banded, grey to dark greyish brown clay. The
224 colour banding varies from a few millimetres (laminae) up to 1 cm (thin bedded) in thickness.

225 Interbedded laminae and thin beds of very fine-grained sand occur sporadically within the
226 section. The colour banding reveals that the sequence is folded, with the degree of contortion
227 of the bedding varying down the core. The most extreme attenuation of the bedding occurs
228 between 2 and 3 m depth where the style of folding is asymmetric, with some limbs partly
229 boudinaged and/or offset by a few millimetres along micro-faults. The intensity of the folding
230 appears to initially decrease below 3 m depth, but increases again below 4.5 m to the base of
231 the core. The operational log of the vibrocorer showed a uniform rate of penetration, and the
232 deformation is regarded as primary rather than an artefact of the coring. Coastal outcrops of
233 these deposits also reveal evidence of small-scale faulting and liquefaction structures (Stoker
234 *et al.* in press). The upper 30 cm of the Assynt Glacigenic Formation is bioturbated, and a
235 sharp, irregular, eroded surface marks its contact with the overlying Outer Loch Broom shell
236 bed.

237

238 **Interpretation and discussion**

239

240 Timing of deformation

241

242 The faults within the Assynt Glacigenic Formation do not extend into the overlying units, and
243 deformation and displacement is therefore regarded as early, post-depositional. The regional
244 stratigraphy of the area suggests that deformation occurred between about 14 and 13 ka BP,
245 during the Lateglacial Interstadial (Fig. 2). BGS sediment core 57-06/269 proved that
246 deformation took place prior to the onset of deposition of the Outer Loch Broom shell bed
247 which, by correlation with the Inner Loch Broom shell bed, is probably no younger than about
248 13 ka BP (Stoker *et al.* in press) (Fig. 5).

249

250 Mechanics of deformation

251

252 The primary sea bed expression of both features A and B is a broad depression between 10
253 and 20 m deep and several hundred metres wide. The seismic reflection and core data indicate
254 that these features have developed in association with faulting and folding of the Assynt
255 Glacigenic Formation. Normal faults predominate, although reverse faulting and folding
256 accompany the development of feature A. The most penetrative faults associated with feature
257 A have a curved, listric style. Bedding is offset by the faults, and at the metre to decimetre
258 scale (the seismic profile) the thickness of beds remains uniform, though some attenuation of
259 laminae and thin beds is observed at the scale of the sediment core. In general, the internal
260 structure of the disturbed section remains coherent. The truncation of reflections at the margin
261 of the depressions may be indicative of post-deformation bottom-current erosion, which
262 possibly enhanced or deepened the depressions prior to the deposition of the overlying
263 Summer Isles Formation (this is discussed further below).

264

265 The structural characteristics are typical of mass movement associated with submarine slides
266 and slumps in prodelta and continental margin settings (Mulder & Cochonat 1996). Rotational
267 failure surfaces are indicative of slumps. The combination of extension and compression
268 associated with feature A is comparable to mass failure described from unconsolidated
269 prodelta sediments commonly observed in both glacial and non-glacial settings (e.g. Coleman
270 *et al.* 1980; Syvitski & Hein 1991), where extension at the headwall is compensated by
271 compression at the toe of the slide. However, in contrast to the prodelta environment, which
272 has a natural depositional slope that facilitates gravity-driven translation and/or rotation, the
273 deformation in Loch Broom is contained wholly within flat-lying basinal sediments.
274 Nevertheless, a similar gravity-driven transport mechanism acting upon the sediments of the

275 Assynt Glacigenic Formation is envisaged, albeit with the extent of displacement severely
276 constrained by the fjord walls.

277

278 In the case of feature A, the direction of displacement appears to have been from the NW to
279 SE within and along the axis of the loch, with the depression, at least in part, related to the
280 folding. However, the rectilinear shape of feature A might imply some degree of controlled
281 collapse of the section leading to a lowering of the sea bed surface. In the absence of a
282 comparable fold pair associated with feature B, it remains uncertain whether or not some
283 other process has contributed to the development of these depressions, such as fluid escape,
284 localised collapse or remobilisation of the basal fill underlying the Assynt Glacigenic
285 Formation, or localised block faulting and subsidence of the bedrock; all of which may have
286 accompanied deformation. Depressions of a comparable scale described from Loch Tay, a
287 freshwater lake in central Scotland, have been attributed to gas escape induced by movement
288 on the Loch Tay Fault (Duck & Herbert 2006). Shallow gas and pockmarks are present in the
289 Summer Isles region, especially in the inner part of Loch Broom (Stoker *et al.* 2006), though
290 there is no evidence for gas (or its former presence) in the outer part of the loch. Fluid seepage
291 (e.g. interstitial pore water) from deeper levels may be driven to the surface by active faults,
292 and commonly results in a mottled sea bed surface resolved as a polygonal pattern (Davies *et*
293 *al.* 1999; Long *et al.* 2004; Trincardi *et al.* 2004). In the study area, the faulted palaeo-sea bed
294 surface generated at the time of deformation in Loch Broom is wholly buried beneath younger
295 sediments; thus, its surface pattern remains uncertain. It cannot be discounted that the broadly
296 rectilinear outline of the depressions could be indicative of a degree of fault-controlled fluid
297 release from the basal fjord deposits, which may have led to their localised collapse.

298

299 Release mechanism

300

301 In a coastal environment, the triggering mechanism is almost always gravity (e.g. sediment
302 loading, wave-induced cyclic loading) or earthquake shaking (Syvitski & Shaw 1995; Mulder
303 & Cochonat 1996). In general terms, gravity alone would require a sloping area in order to
304 facilitate a mass transfer of sediment downslope, e.g. oversteepening of a delta front. In
305 contrast, earthquake shock can result in the sudden loss of sediment strength associated with
306 the upward movement of pore fluid. Shallow soft sediments are especially prone to the
307 amplification of earthquake ground motion (Jackson *et al.* 2004). Thus, basin-floor sediments
308 may be as equally susceptible to physical disturbance and failure during earthquake loading,
309 as those on the adjacent slopes. On this basis, we suggest that earthquake activity is most
310 likely the primary release mechanism involved in the deformation of the Assynt Glacigenic
311 Formation basinal deposits in Loch Broom.

312

313 Implications for Lateglacial instability in the Summer Isles region

314

315 In the adjacent North Annat Basin, the Cadail Slide (Fig. 1) was also activated in the interval
316 14–13 ka BP; failure of the Assynt Glacigenic Formation sediments occurred prior to the
317 deposition of the Annat Bay Formation, which onlaps the slide deposits (Stoker *et al.* in press)
318 (Fig. 2; Table 1). Collectively, the broad coincidence in the timing of deformation in Loch
319 Broom and the North Annat Basin suggests that these failures may be the expression of a
320 regional instability event. In Little Loch Broom, a series of slides and slumps comprise the
321 Little Loch Broom Slide Complex (Wilson *et al.* in press), which has also reworked the
322 Assynt Glacigenic Formation. This is the largest area of focused mass failure in the Summer
323 Isles region. Although the age of the slide complex remains ambiguous, it has been tentatively
324 assigned to the same instability event as the Cadail Slide and the Loch Broom basinal features

325 on the basis of its comparable scale and magnitude. It should be noted that unequivocal
326 Holocene failures within Little Loch Broom (Fig. 1) are much smaller in scale, affect only the
327 Summer Isles Formation, and are commonly either the result of plastic flow or turbidity
328 currents (Wilson *et al.* in press).

329

330 Neotectonic activity linked to glacio-isostatic rebound is a well established phenomenon
331 along the Atlantic continental margin of NW Europe. On the SW Norwegian margin, a
332 detailed study of the giant Storrega Slide concluded that a major seismic pulse most likely
333 accompanied deglaciation (Evans *et al.* 2002; Bryn *et al.* 2003; Haflidason *et al.* 2004).

334 Differential rebound following ice unloading is also known to reactivate pre-existing
335 structural lineaments and bedrock weaknesses as the new stress regime is accommodated.

336 Enhanced seismicity along the coastal areas of northern, western and southeastern Norway is
337 an established fact, and earthquake-triggered tsunami waves in fjords continue to constitute a
338 major present-day seismic hazard to Norwegian society (Olesen *et al.* 2008). In the UK, the
339 late to earliest postglacial reactivation of pre-existing Caledonian and older lineaments is
340 known to have generated normal faulting with metre-scale displacement in the southern
341 Sperrin Mountains, in Northern Ireland (Knight 1999). Late to postglacial reactivation has
342 also resulted in movement on faults, such as the Kinloch Hourn Fault, in western Scotland
343 (Stewart *et al.* 2001), possibly the Loch Tay Fault in central Scotland (Duck & Herbert 2006),
344 and caused liquefaction of lake sediments in the former ice-dammed lake at Glen Roy
345 (Ringrose 1989). Consequently, it seems reasonable to infer that palaeoseismic activity was
346 also occurring in the Summer Isles region during Lateglacial time, especially as the west coast
347 of Scotland, from Ullapool southwards, continues to be a major focus for earthquakes at the
348 present-day (Musson 2003). It may be no coincidence that all three areas of major

349 deformation in the Summer Isles region are most probably located along lines of NW-
350 trending faults (Fig. 1).
351
352 Origin of the discrete hollows in feature B
353
354 Superficially, the hollows developed within feature B resemble pockmarks on the swath
355 bathymetry image; however, inspection of seismic profile 05/04-47 reveals a different origin
356 related wholly to the origin of the Summer Isles Formation. Regional mapping of this unit
357 indicates that its deposition has been strongly influenced by the action of bottom currents
358 (Stoker *et al.* in press). Features that result from bottom-current activity include the localised
359 depositional build-up of sediment drifts and associated erosional scours and moats, especially
360 where there is a change in bathymetry, e.g. base of a slope or in pre-existing depressions
361 (Stow *et al.* 2002). Localised erosion within features A and B is implied by the truncated
362 reflections on their margin (Figs 4b & 4c). Core data from inner Loch Broom suggest that the
363 basal infill in both depressions may represent a high-energy fill associated with this erosional
364 process (Stoker *et al.* in press). Stabilisation of the bottom-current flow is reflected by the
365 subsequent deposition and moulding of the acoustically layered sediments of the Summer
366 Isles Formation.
367
368 Bedforms generated by differential deposition and erosion are common throughout the
369 Summer Isles region. One of the best examples is observed at the southeast end of the inner
370 part of outer Loch Broom where a sediment drift and moat are well developed within the
371 Summer Isles Formation, at the point where the sea bed begins to shallow towards Ullapool
372 (Fig. 4a). These bedforms are generally the result of helical flow of the bottom current
373 adjacent and parallel to the slope, which creates enhanced erosion at the base of the flow

374 underlying the core of the current, leading to deposition on the downslope flank of the flow
375 where bottom-current velocity is reduced. The geometry of the Summer Isles Formation
376 within feature B (Fig. 4b) reflects such differential sedimentation set up by a complex
377 perturbation in bottom-current flow caused by the depression; the hollows represent erosional
378 moats or scours separated by the depositional build-up of the drift deposit within the
379 depression (Fig. 4). This is comparable to the ‘infill drift’ style of Stow *et al.* (2002), which is
380 commonly found as infills or partial infills at the head of a slump scar, or at the margins and
381 toe region of a slump/slide mass.

382

383 **Conclusions**

384

- 385 • Swath bathymetry and seismic reflection profiles in outer Loch Broom have revealed
386 slumping within the basin-floor fjord deposits of the Assynt Glacigenic Formation. At the
387 sea bed, the effect of slumping is manifest as two distinct depressions between 10 and 20
388 m deep and 350 m wide. Below the sea bed, it is observed that slumping has been
389 accommodated along rotational faults. In feature A, displacement has been to the
390 southeast, along the axis of the loch, with localised compression in the toe region causing
391 a broad, low-amplitude uplift of the sea bed. The possibility that collapse of the sea bed
392 has been partly facilitated by some kind of associated fluid release along the fault planes
393 cannot be discounted.
- 394 • Sediment core data indicate that deformation of the Assynt Glacigenic Formation
395 occurred early post-depositional, prior to the deposition of the Outer Loch Broom shell
396 bed at about 13 ka BP. This is consistent with the regional stratigraphy, which indicates
397 that the Assynt Glacigenic Formation was deposited between about 14 and 13 ka BP,
398 during the deglaciation of the fjord region.

- 399 • It is inferred that the slumping event in Loch Broom correlates broadly with two other
400 major slides in the region, the Cadail Slide and the Little Loch Broom Slide Complex.
401 Collectively, these mass failures may be indicative of a phase of regional instability
402 during the Lateglacial interval. It is concluded that earthquake activity linked to glacio-
403 isostatic unloading is the most probable cause of this instability.
- 404 • Bottom-current activity eroded the original surface of the depressions, which have been
405 partially to almost totally infilled as the bottom currents stabilised, enabling the deposition
406 of the Holocene Summer Isles Formation.

407

408 **Acknowledgements**

409

410 The authors would like to thank the masters and crew of the *R/V Calanus* and *R/V James*
411 *Cook* for their skill and assistance during the collection of the geophysical and geological
412 datasets. We thank David Long, Alan Stevenson and an anonymous referee for comments on
413 an earlier version of this manuscript. Published with the permission of the Executive Director,
414 BGS (NERC).

415

416 **References**

- 417 AARSETH, I.A., LØNNE, O. & GISKEØDEGAARD, O. 1989. Submarine slides in
418 glaciomarine sediments in some western Norwegian fjords. *Marine Geology*, **88**, 1–21.
- 419 BRADWELL, T., FABLE, D., STOKER, M.S., MATHERS, H., MCHARGUE, L. & HOWE,
420 J.A. 2008. Ice caps existed throughout the Lateglacial Interstadial in northern Scotland.
421 *Journal of Quaternary Science*, **23**, 401–407.

422 BRITISH GEOLOGICAL SURVEY. 1998. *Summer Isles. Scotland Sheet 101W. Solid and*
423 *Drift Geology. 1:50 000 Provisional Series.* (Keyworth, Nottingham: British Geological
424 Survey).

425 BRYN, O., SOLHEIM, A., BERG, K., LIEN, R., FORSBERG, C.F., HAFLIDASON, H.,
426 OTTESEN, D. & RISE, L. 2003. The Storegga Slide complex; repeated large scale sliding
427 in response to climate cyclicality. *In* LOCAT, J. & MIENERT, J. (eds) *Submarine Mass*
428 *Movements and their Consequences*, Kluwer Academic Publishing, Netherlands, 215–222.

429 COLEMAN, J.M., PRIOR, D.B. & GARRISON, L.E. 1980. *Subaqueous Sediment*
430 *Instabilities in the Offshore Mississippi River Delta.* Bureau of Land Management, New
431 Orleans, Open File Report 80-01.

432 DAVIES, R., CARTWRIGHT, J. & RANA, J. 1999. Giant hummocks in deep-water
433 sediments – evidence for large scale differential compaction and density inversion during
434 early burial. *Geology*, **27**, 907–910.

435 DUCK, R.W. & HERBERT, R.A. 2006. High-resolution shallow seismic identification of gas
436 escape features in the sediments of Loch Tay, Scotland: tectonic and microbiological
437 associations. *Sedimentology*, **53**, 481–493.

438 EVANS, D., MCGIVERON, S., HARRISON, Z., BRYN, P. & BERG, K. 2002. Along-slope
439 variation in the late Neogene evolution of the mid-Norwegian margin in response to uplift
440 and tectonism. *In* DORÉ, A.G., CARTWRIGHT, J.A., STOKER, M.S., TURNER, J.P. &
441 WHITE, N. (eds) *Exhumation of the North Atlantic Margin: Timing, Mechanisms and*
442 *Implications for Petroleum Exploration.* Geological Society, London, Special
443 Publications, **196**, 139–151.

444 FAIRBANKS, R.G., MORTLOCK, R.A., CHIU, T.C., KAPLAN, A., GUILDERSON, T.P.,
445 FAIRBANKS, T.W. & BLOOM, A.L. 2005. Marine radiocarbon calibration curve

446 spanning 0 to 50,000 years B.P. based on paired $^{230}\text{Th}/^{234}\text{U}/^{238}\text{U}$ and ^{14}C dates on pristine
447 corals. *Quaternary Science Reviews*, **24**, 1781–1796.

448 HAFLIDASON, H., SEJRUP, H.P., NYGÅRD, A., MIENERT, J., BRYN, P., LIEN, R.,
449 FORSBERG, C.F., BERG, K. & MASSON, D. 2004. The Storegga Slide: architecture,
450 geometry and slide development. *Marine Geology*, **213**, 201–234.

451 HAMILTON, E.L. 1985. Sound velocity as a function of depth in marine sediments. *Journal*
452 *of the Acoustic Society of America* **78**, 1348–1355.

453 HJELSTUEN, B.O., HAFLIDASON, H., SEJRUP, H.P. & LYSÅ, A. 2009. Sedimentary
454 processes and depositional environments in glaciated fjord systems – Evidence for
455 Nordfjord, Norway. *Marine Geology*, doi:10.1016/j.margeo.2008.11.010.

456 JACKSON, P.D., GUNN, D.A. & LONG, D. 2004. Predicting variability in the stability of
457 slope sediments due to earthquake ground motion in the AFEN area of the western UK
458 continental shelf. *Marine Geology*, **213**, 363–378.

459 KNIGHT, J. 1999. Geological evidence for neotectonic activity during deglaciation of the
460 southern Sperrin Mountains, Northern Ireland. *Journal of Quaternary Science*, **14**, 45–57.

461 LONG, D., BULAT, J. & STOKER, M.S. 2004. Sea bed morphology of the Faroe-Shetland
462 Channel derived from 3D seismic datasets. In DAVIES, R.J., CARTWRIGHT, J.A.,
463 STEWART, S.A., LAPPIN, M. & UNDERHILL, J.R. (eds) *3D Seismic Technology:*
464 *Application to the Exploration of Sedimentary Basins*. Geological Society, London,
465 *Memoirs*, **29**, 53–61.

466 McQUILLIN, R. & ARDUS, D.A. 1977. *Exploring the Geology of Shelf Seas*. Graham &
467 Trotman Limited, London.

468 MULDER, T. & COCHONAT, P. 1996. Classification of offshore mass movements. *Journal*
469 *of Sedimentary Research*, **66**, 43–57.

- 470 MUSSON, R. 2003. *Seismicity and Earthquake Hazard in the UK*. British Geological Survey:
471 http://www.quakes.bgs.ac.uk/hazard/Hazard_UK.htm.
- 472 NIESSEN, F. & WHITTINGTON, R.J. 1997. Synsedimentary faulting in an East Greenland
473 Fjord. In DAVIES, T.A., BELL, T., COOPER, A.K., JOSEPHANS, H., POLYAK, L.,
474 SOLHEIM, A., STOKER, M.S. & STRAVERS, J.A. (eds) *Glaciated Continental*
475 *Margins: An Atlas of Acoustic Images*, Chapman & Hall, London, 130–131.
- 476 OLESEN, O., BUNGUM, H., DEHLS, J., LINDHOLM, C., PASCAL, C. & ROBERTS, D.
477 2008. Neotectonics in Norway – mechanisms and implications. Abstract: International
478 Geological Congress, Oslo, 2008. Available at:
479 <http://www.cprm.gov.br/33IGC/1398408.html>.
- 480 RINGROSE, P.S. 1989. Palaeoseismic (?) liquefaction event in late Quaternary lake sediment
481 at Glen Roy, Scotland. *Terra Nova*, **1**, 57–62.
- 482 SANGREY, D.A., CORNELL, U., CLUKEY, E.C. & MOLNIA, B.F. 1979. Geotechnical
483 engineering analysis of underconsolidated sediments from Alaska coastal waters. 11th
484 Offshore Technology Conference, Houston, 1: 677–682.
- 485 STEWART, I.S., FIRTH, C.R., RUST, D.J., COLLINS, P.E.F. & FIRTH, J.A. 2001.
486 Postglacial fault movement and palaeoseismicity in western Scotland: A reappraisal of the
487 Kinloch Hourn fault, Kintail. *Journal of Seismology*, **5**, 307–328.
- 488 STOKER, M.S., LESLIE, A.B., SCOTT, W.D., BRIDEN, J.C., HINE, N.M., HARLAND, R.,
489 WILKINSON, I.P., EVANS, D. & ARDUS, D.A. 1994. A record of late Cenozoic
490 stratigraphy, sedimentation and climate change from the Hebrides Slope, NE Atlantic
491 Ocean. *Journal of the Geological Society, London* **151**, 235–249.
- 492 STOKER, M.S., BRADWELL, T., WILSON, C., HARPER, C., SMITH, D. & BRETT, C.
493 2006. Pristine fjord landsystem revealed on the sea bed in the Summer Isles region, NW
494 Scotland. *Scottish Journal of Geology*, **42**, 89–99.

495 STOKER, M.S., BRADWELL, T., HOWE, J.A., WILKINSON, I.P. & MCINTYRE, K. In
496 press. Lateglacial ice-cap dynamics: evidence from the fjords of NW Scotland.
497 *Quaternary Science Reviews*.

498 STOW, D.A.V., FAUGÈRES, J.-C., HOWE, J.A., PUDSEY, C.J. & VIANA, A.R. 2002.
499 Bottom currents, contourites and deep-sea sediment drifts: current state of the art. In
500 STOW, D.A.V., PUDSEY, C.J., HOWE, J.A., FAUGÈRES, J.-C. & VIANA, A.R (eds)
501 *Deep-Water Contourite Systems: Modern Drifts and Ancient Series, Seismic and*
502 *Sedimentary Characteristics*. Geological Society, London, Memoirs, **22**, 7–20.

503 SYVITSKI, J.P.M. & HEIN, F.J. 1991. *Sedimentology of an Arctic Basin: Itirbilung Fiord,*
504 *Baffin Island, Northwest Territories*. Geological Survey of Canada Paper 91-11.

505 SYVITSKI, J.P.M. & SHAW, J. 1995. Sedimentology and Geomorphology of Fjords. In
506 PERILLO, G.M.E. (ed) *Geomorphology and Sedimentology of Estuaries. Developments in*
507 *Sedimentology* 53, Elsevier Science BV, Amsterdam, 113–178.

508 TRINCARDI, F., CATTANEO, A., CORREGGIARI, A. & RIDENTE, D. 2004. Evidence of
509 soft sediment deformation, fluid escape, sediment failure and regional weak layers within
510 the late Quaternary mud deposits of the Adriatic Sea. *Marine Geology*, **213**, 91–119.

511 WHITTINGTON, R.J. & NIESSEN, F. 1997. Staircase rotational slides in an ice-proximal
512 fjord setting, East Greenland. In DAVIES, T.A., BELL, T., COOPER, A.K.,
513 JOSENHANS, H., POLYAK, L., SOLHEIM, A., STOKER, M.S. & STRAVERS, J.A.
514 (eds) *Glaciated Continental Margins: An Atlas of Acoustic Images*, Chapman & Hall,
515 London, 132–133.

516 WILSON, C.R., STOKER, M.S., HOWE, J.A., BRADWELL, T. & LONG, D. In press. Slope
517 instability in Scottish fjords: an example from Little Loch Broom. In AUSTIN, W.E.N.,
518 HOWE, J.A., FORWICK, M., POWELL, R. & PAETZEL, M. (eds) *Fjordic Depositional*
519 *Systems*. Geological Society, London, Special Publications.

1 **Table caption**

2

- 3 1. Interpretation of Late Quaternary stratigraphic units in the Summer Isles region (after
4 Stoker *et al.* in press).

5

6 **Figure captions**

7

- 8 1. Location of study area, which is expanded in Fig. 3, in relation to regional structural grain.
9 Occurrences of other areas of mass failure cited in text are also shown: C, Cadail Slide; H,
10 Holocene failures; LLB, Little Loch Broom Slide Complex. Other abbreviations: GI,
11 Gruinard Island; NAB, North Annat Basin.
- 12 2. Late Quaternary stratigraphic scheme for the Summer Isles region (simplified from Stoker
13 *et al.* in press), including inferred relative timing of neotectonic events.
- 14 3. Swath bathymetric image showing sea bed depressions in outer Loch Broom: a)
15 perspective view (see b for scale bar) looking NW from Ullapool towards Cadail Bank at
16 mouth of loch; b) planform view with interpreted map. Seismic profiles shown in Figs 4a–
17 4c.
- 18 4. Seismic reflection profiles across features A and B (see text for details). a) Interpreted line
19 drawing of part of BGS boomer profile 05/04-37 showing the disposition of the Late
20 Quaternary units in outer Loch Broom. Inset shows sub-bottom detail of feature A and
21 associated faults and folds; b) Interpretation of profile 05/04-48 across feature A; c)
22 Interpretation of profile 05/04-47 across feature B. Inset map shows location of profiles.
23 Abbreviations: BT, bottom tracking indicator; M, moat; RA, rollover anticline; SD,
24 sediment drift; TR, truncated reflections.

25 5. Graphic log of BGS core 57-06/269 from outer Loch Broom, focusing on the sedimentary
26 structure of the Assynt Glacigenic Formation, especially the within-core variation in the
27 style and intensity of deformation of the laminated sediment. Core is located in Figs 3 and
28 4.
29

Table 1

Stratigraphic unit	Depositional setting
Summer Isles Fm	Marine deposits strongly influenced by bottom currents. Localised mass failure
Ullapool Gravel Fm	Fluvioglacial outwash fan-deltas
Inner and Outer Loch Broom shell beds	Time-transgressive condensed section in Loch Broom
Late-stage debris flows	Discrete, localised debris-flow deposits
Annat Bay Fm	Distal glacimarine facies, diachronous with Assynt Glacigenic Fm
Assynt Glacigenic Fm (including Late-stage members)	Recessional, oscillating, ice-contact and proximal glacimarine facies. Contemporaneous mass failure, e.g. Little Loch Broom slide complex; Cadail slide (pre-Annat Bay Fm); neotectonic deformation in Loch Broom
Loch Broom Till Fm	Subglacial lodgement till

Fig 1

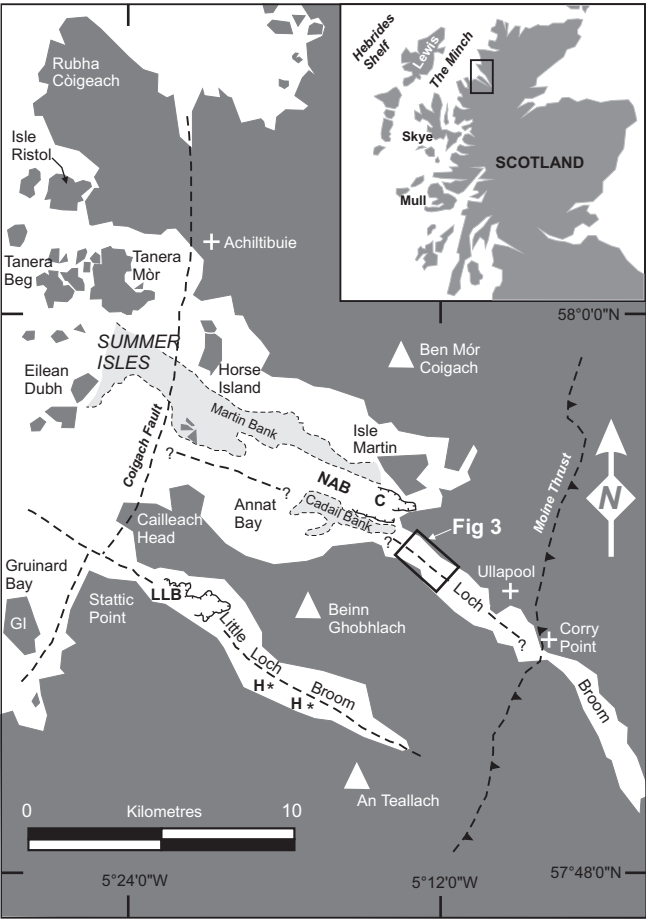


Fig 2

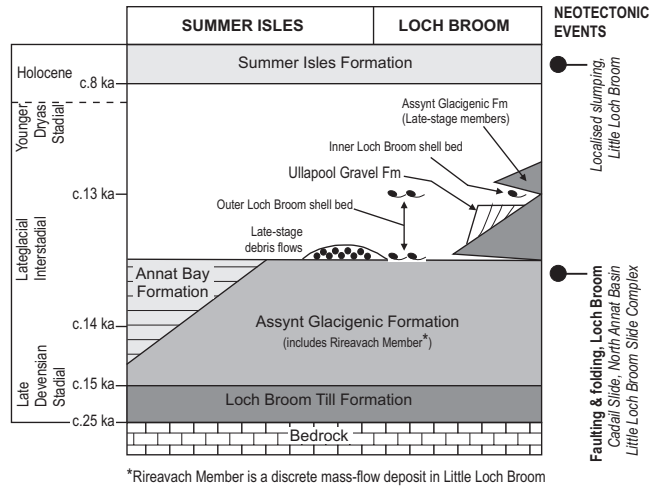
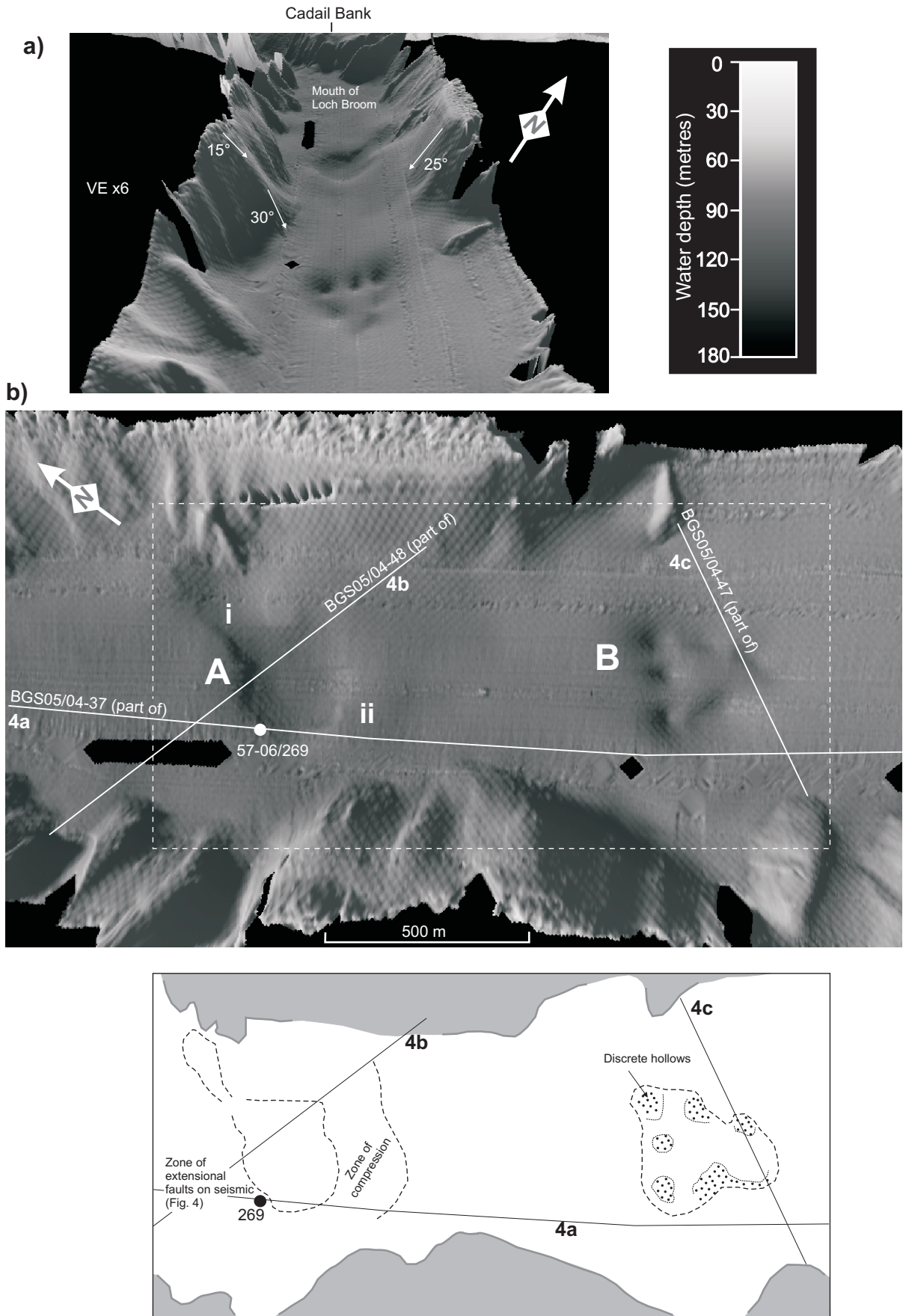


Fig 3



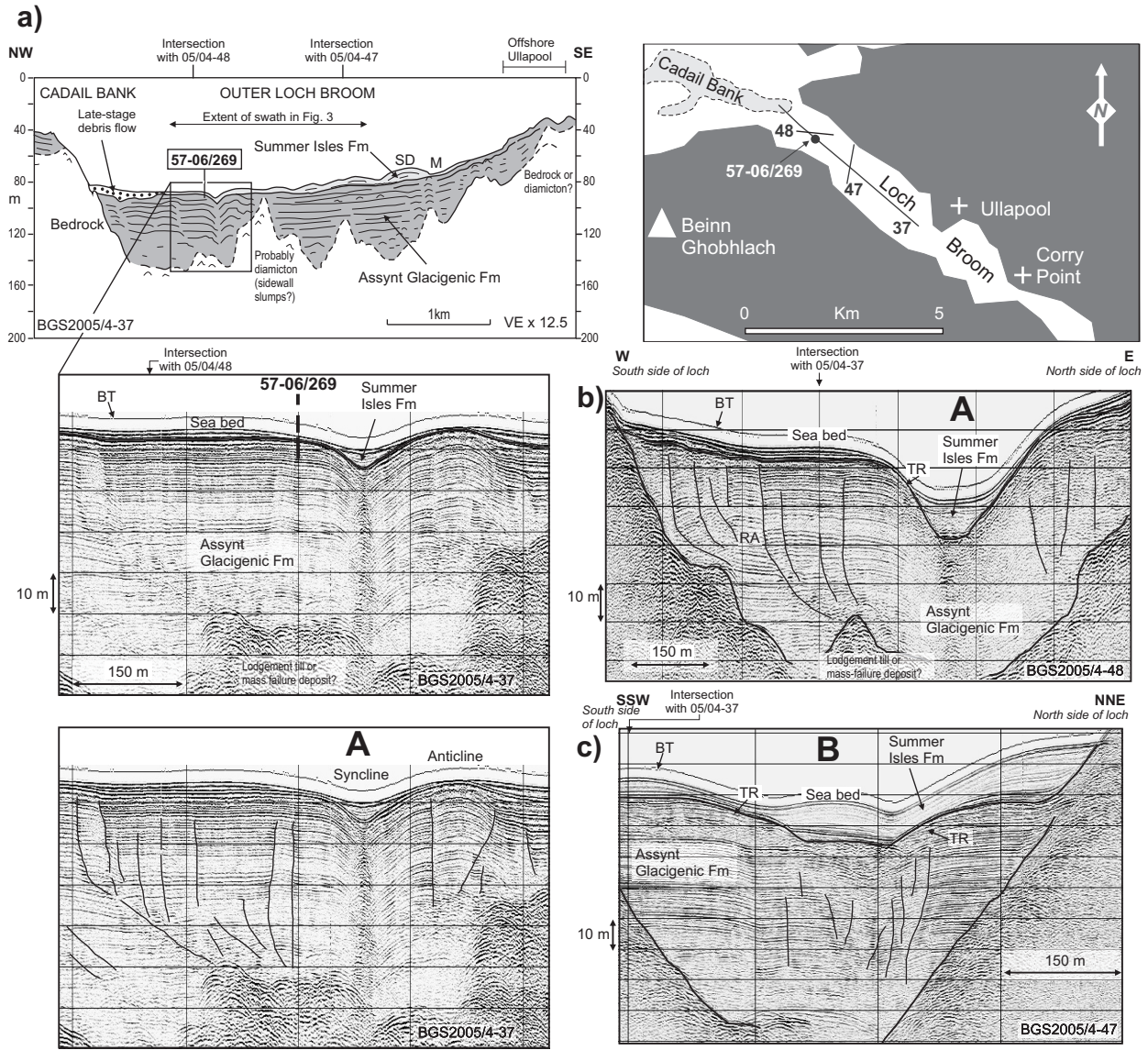


Fig 5

